Accepted version of: Heinrich Edgar Arnold Laue and Warren Paul du Plessis, “A Checkered Network for Implementing Arbitrary Overlapped Feed Networks,” *IEEE Transactions on Microwave Theory and Techniques*, vol. 67, no. 11, pp. 4632–4640, Nov. 2019. DOI: 10.1109/TMTT.2019.2940223

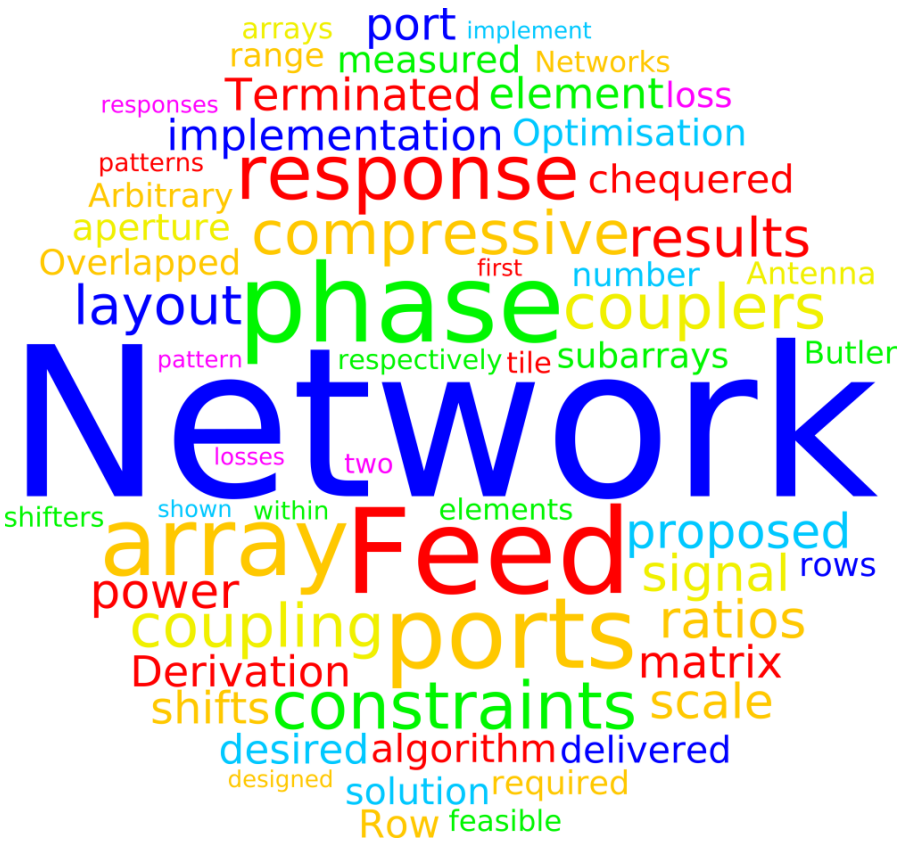

ABBREVIATIONS

CS	compressive sensing
CSIR	Council for Scientific and Industrial Research
DFT	discrete Fourier transform
FFT	fast Fourier transform
LNA	low-noise amplifier
NRF	National Research Foundation of South Africa
RFIC	radio-frequency integrated circuit
SLL	sidelobe level
SQP	sequential quadratic programming
ULA	uniform linear array
VSWR	voltage standing wave ratio

A Chequered Network for Implementing Arbitrary Overlapped Feed Networks

Heinrich Edgar Arnold Laue, *Student Member, IEEE,* and Warren Paul du Plessis, *Senior Member, IEEE*

***Abstract*—Existing overlapped subarray techniques for beamforming arrays aim to realise flat-topped subarray radiation patterns, where pattern synthesis is constrained by the hardware configuration. A generalised framework for designing compressive arrays with unconstrained feed network responses has recently been proposed with promising results, but no hardware implementation has been proposed. A planar chequered network of directional couplers and fixed phase shifters is proposed for implementing arbitrary complex-valued feed network responses, including completely overlapped networks. An algorithm is proposed for realising a desired response while minimising the range of coupling ratios and phase shifts required. The technique is validated by a comparison to the standard 4 × 4 Butler matrix implementation, and its versatility illustrated by sharing an 8-element aperture between three independently designed non-scanning arrays. A manufactured microstrip 2 × 4 compressive array feed network achieves the desired aperture illuminations to within 0.6 dB and 5.2° at 3.15 GHz, and to within 1.4 dB and 10.3° across the impedance bandwidth of 4.5%.**

***Index Terms*—Antenna feed networks, subarrays, beam steering, phased arrays, Butler matrices**

I. Introduction

SUBARRAYS take weighted combinations of antenna-element signals so that each subarray spans multiple antenna elements [1]–[5]. The array aperture is shared between the subarrays, and each subarray has a unique radiation pattern. The subarrays can be combined to perform beamforming by connecting a beamforming control (a phase shifter, receiver, or transmitter) to each subarray. There are typically more antenna elements than subarrays, leading to reduced-control arrays [5]. More elements allow greater control over the subarray patterns [5]. Often, the steering range is limited to allow high-directivity beams to be steered over relatively small angular ranges. Nulls may also be placed in the subarray patterns to suppress interferers before sampling [5].

Subarrays may be non-overlapping/contiguous, partially overlapped, or completely overlapped [1]–[3], [6], [7]. Each antenna element is connected to only one subarray in the non-overlapping case, while each subarray output is a function of all antenna-element signals in the completely-overlapped case. The partially-overlapped case is a compromise between these two extremes with some elements being shared between subarrays. Completely overlapped subarrays present the greatest control over the subarray patterns [2], [5].

Various feed network layouts exist for implementing overlapped feed networks using couplers, crossovers, lenses, and/or reflectors [1]–[3]. Overlapped feed networks have successfully been manufactured using stripline [8], [9], waveguide [3], lenses [10], and radio-frequency integrated circuits (RFICs) [11].

Traditionally, subarray pattern synthesis is linked to the chosen feed network layout, where the aim is to synthesise flat-topped subarray patterns for a limited steering range [1]–[4]. Recently, a generalised framework for designing compressive feed networks for beamforming arrays was proposed [5], allowing both arbitrary sidelobe specifications and the ability to constrain the subarray patterns outside the steering range. The compressive array design algorithm [5] synthesises a complex-valued feed network response which meets the pattern amplitude specifications, and has been shown to obtain lower sidelobe level (SLL) than a dual-transform [1] subarray system [5]. No details on how such arrays could be physically implemented were provided and no hardware constraints were placed on the feed network response.

The problem of implementing an arbitrary complex-valued feed network response is addressed below by presenting a novel overlapped feed network layout consisting of interconnected couplers and fixed phase shifters. Arbitrary responses are allowed in the sense that no constraints are applied to the feed network responses to be implemented, enabling the full exploitation of compressive arrays. The proposed approach therefore separates the tasks of subarray pattern synthesis and feed network implementation.

While no constraints are placed on the feed network response to be implemented, constraints may be placed on the coupling ratios and phase shifts to ensure realisability. An algorithm is proposed below to implement a desired feed network response while minimising the range of coupling ratios and phase shifts required. Constraints may also be

Manuscript received 13 Nov. 2018; revised 11 Feb. 2019; accepted 21 Jul. 2019.

This work is based on the research supported in part by the National Research Foundation of South Africa (NRF) (Grant specific unique reference number (UID) 85845). The NRF Grantholder acknowledges that opinions, findings and conclusions or recommendations expressed in any publication generated by the NRF supported research are that of the author(s), and that the NRF accepts no liability whatsoever in this regard.

The authors are with the Department of Electrical, Electronic and Computer Engineering, University of Pretoria, Pretoria 0002, South Africa (e-mail: laueheinrich@gmail.com; wduplessis@ieee.org)

This paper has supplementary downloadable material available at http://ieeexplore.ieee.org, provided by the authors. This includes the chequered network design algorithm, tested in MATLAB R2018b, for generating the results in this paper. This material is 48 kB in size.

Color versions of one or more of the figures are available online at http://ieeexplore.ieee.org.

Digital Object Identifier 00.0000/TMTT.0000.000000

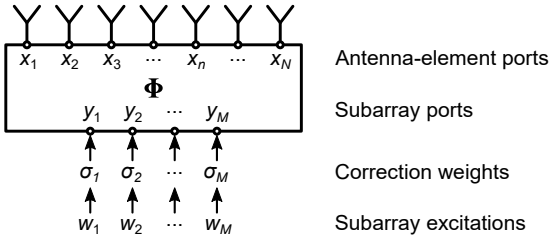

Fig. 1. A generalised overlapped feed network.

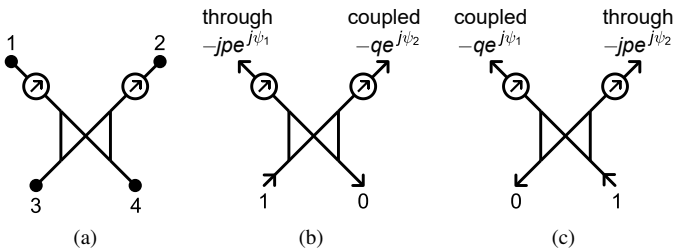

Fig. 2. Definition of a single tile consisting of a directional coupler and two fixed phase shifters: (a) Tile port definitions. (b) Tile response to a stimulus at port 3. (c) Tile response to a stimulus at port 4.

placed on the power delivered to terminations to reduce losses.

Section II introduces the proposed chequered feed network layout and presents a method for deriving its response. Section III presents an algorithm for designing the feed network to implement a desired response. Section IV presents results for some test cases, including measured results for a microstrip implementation of a compressive array with 4 antenna elements and 2 subarrays. A summary of the main results is provided in Section V.

II. The Chequered Network Layout for Arbitrary Feed Network Responses

A. Overlapped Feed Networks

An arbitrary overlapped feed network with M subarrays for N antenna elements is illustrated in Fig. 1. On reception, the feed network can be described by the equation $\mathbf{y} = \mathbf{\Phi x}$, where $\mathbf{x}$ is the $N \times 1$ vector of signals at the N antenna elements, $\mathbf{\Phi}$ is an $M \times N$ complex-valued matrix describing the feed network response, and $\mathbf{y}$ is the $M \times 1$ vector of transformed signals at the M subarray ports [5]. Row m of $\mathbf{\Phi}$ describes how the N antenna-element signals are weighted and combined to form the output of the mth subarray. Equivalently, row m of $\mathbf{\Phi}$ describes the aperture illumination at the antenna elements produced by the mth subarray on transmission. Different beam patterns can be achieved by varying the signals applied to the subarrays using transmitters, receivers, amplifiers, attenuators and/or variable phase shifters.

A feed network is completely overlapped if each subarray output is a function of all the antenna-element signals, which leads to a fully populated $\mathbf{\Phi}$ [5]. A contiguous feed network will have a $\mathbf{\Phi}$ with only one non-zero entry per column, and a partially overlapped feed network will have at least one zero entry per row in $\mathbf{\Phi}$. Ports are labelled according to their signal variables, so antenna-element ports are labelled x_1 to x_N and subarray ports y_1 to y_M as shown in Fig. 1. Terminated ports are labelled z_l, where $l \in 1, \ldots, T$, and T is the number of terminated ports which depends on the chosen layout.

B. The Chequered Layout

The proposed network uses a tile consisting of a directional coupler and two fixed phase shifters as its basic element, as illustrated and defined in Fig. 2, with reciprocity applying. The specific coupler used here is a single-section branchline coupler [12], although the technique is also applicable to other couplers with similar port layouts. The phase shifters are fixed and their simplest implementation is varying lengths of transmission line, although other phase shifters with wider bandwidths can also be employed. The relative power delivered to the through and coupled port is p^2 and q^2, respectively, with $p^2+q^2 = 1$. The coupling ratio is defined as p/q. Coupling ratios above and below 0 dB indicate more power being transferred to the through and coupled ports, respectively. A coupling ratio of 0 dB indicates an equal-split coupler.

The tiles are connected in a chequered pattern to form the feed network, similar to the way couplers are connected in the chess network proposed by Skobelev [3], [13]. The layout is planar and requires no physical crossovers. Each row of couplers is identical in Skobelev's chess network, whereas the network proposed here allows the parameters of each tile to be specified independently. The top row of tiles connects to the N antenna-element ports, x_n, and the bottom row connects to the M subarray ports, y_n. All remaining tile ports, z_l, have matched terminations. Sufficient rows are required to ensure that there is at least one signal path from each subarray port to each element port when complete overlap is required. This leads to a diamond-shaped chequered layout as illustrated in Fig. 3 for $M = 4$ and $N = 6$, with the minimum number of rows to allow complete overlap being 4. Also shown are the additional tiles required to extend the layout to 5 rows.

The minimum number of rows that achieves the desired overlap between subarrays does not guarantee sufficient degrees of freedom to implement the desired feed network response. The number of rows should thus be increased until the desired response can be realised. A procedure for finding the minimum number of rows required to implement a desired feed network response is outlined in Section III-A.

Typically, there will be two or more signal paths between any subarray and element port. For a stimulus at a given subarray port, the various signal paths to a given element port combine via superposition to produce the desired output. The application of both amplitude and phase alterations along the signal paths allows arbitrary complex-valued responses to be realised as long there are enough tile rows to provide the required degrees of freedom.

It is assumed that arbitrary complex-valued excitations, w_1 to w_M, can be applied to the subarray ports. These variable excitations both allow beamforming even though the feed network itself is fixed, and add additional degrees of freedom which can be exploited to help achieve the required response with the smallest number of tiles.

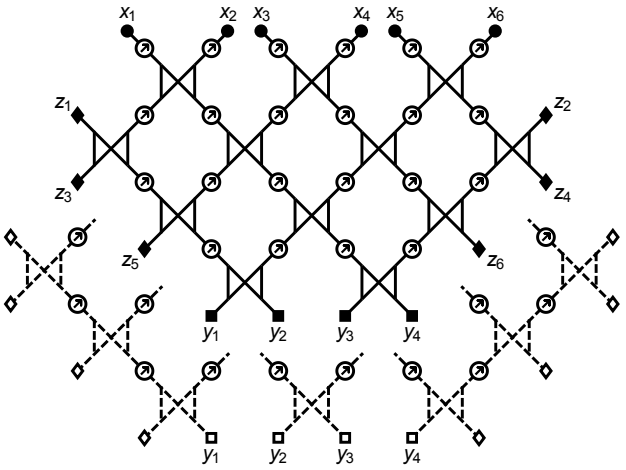

Fig. 3. An example of the proposed network of couplers and fixed phase shifters for $M = 4$ and $N = 6$ and 4 tile rows, with the additional tiles required for extending the layout to 5 rows shown in dashed lines.

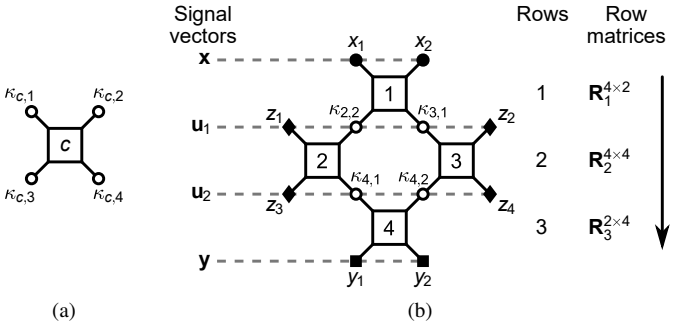

Fig. 4. Derivation of a 2×2 chequered network: (a) Tile symbol with associated intermediate signal variables. (b) Layout with numbered tiles and intermediate signal nodes. The arrow indicates the signal flow convention used to define the row transform matrices.

C. Derivation of the Network Response

The response of a 2×2 network with three rows is derived below, leading to a procedure for deriving the response of any chequered network.

Fig. 4(a) presents a symbol for a tile of the form shown in Fig. 2 along with definitions for the intermediate signals at its ports. The signals flow in a downward direction in Fig. 4(a) when stimuli are applied at $\kappa_{c,1}$ and $\kappa_{c,2}$. The response of tile c can be expressed in matrix form as

$$\begin{bmatrix} \kappa_{c,3} \\ \kappa_{c,4} \end{bmatrix} = \begin{bmatrix} -jp_c e^{j\psi_{c,1}} & -q_c e^{j\psi_{c,2}} \\ -q_c e^{j\psi_{c,1}} & -jp_c e^{j\psi_{c,2}} \end{bmatrix} \begin{bmatrix} \kappa_{c,1} \\ \kappa_{c,2} \end{bmatrix} \quad (1)$$

$$= \mathbf{K}_c \begin{bmatrix} \kappa_{c,1} \\ \kappa_{c,2} \end{bmatrix} \quad (2)$$

where $\mathbf{K}_c$ is the response matrix for tile c. When a node $\kappa_{c,1}$ or $\kappa_{c,2}$ is connected to a terminated port, the corresponding phase shift $\psi_{c,1}$ or $\psi_{c,2}$ is set to zero since it has no effect on the feed network response.

Fig. 4(b) shows a 2×2 chequered layout with intermediate signal nodes, inter-row signal vectors, and row transform matrices that will be used in the derivation to follow. The response will first be derived for stimuli applied to the element ports so that signal flow is in the indicated downward direction.

The inter-row signal vector $\mathbf{u}_1$ is defined as the terminated and inter-tile signals between the first and second rows, and is given by

$$\mathbf{u}_1 = \begin{bmatrix} z_1 \\ \kappa_{2,2} \\ \kappa_{3,1} \\ z_2 \end{bmatrix} = \begin{bmatrix} 0 & 0 \\ -jp_1 e^{j\psi_{1,1}} & -q_1 e^{j\psi_{1,2}} \\ -q_1 e^{j\psi_{1,1}} & -jp_1 e^{j\psi_{1,2}} \\ 0 & 0 \end{bmatrix} \begin{bmatrix} x_1 \\ x_2 \end{bmatrix} \quad (3)$$

$$= \begin{bmatrix} \mathbf{0}_{1\times 2} \\ \mathbf{K}_1 \\ \mathbf{0}_{1\times 2} \end{bmatrix} \mathbf{x} = \mathbf{R}_1 \mathbf{x}. \quad (4)$$

where $\mathbf{0}_{a\times b}$ is an $a \times b$ matrix of zeros, and the row transform matrix for row r is denoted $\mathbf{R}_r$. The next inter-row signal vector $\mathbf{u}_2$ is found to be

$$\mathbf{u}_2 = \begin{bmatrix} z_3 \\ \kappa_{4,1} \\ \kappa_{4,2} \\ z_4 \end{bmatrix} = \begin{bmatrix} \mathbf{K}_2 & \mathbf{0}_{2\times 2} \\ \mathbf{0}_{2\times 2} & \mathbf{K}_3 \end{bmatrix} \begin{bmatrix} z_1 \\ \kappa_{2,2} \\ \kappa_{3,1} \\ z_2 \end{bmatrix} = \mathbf{R}_2 \mathbf{u}_1. \quad (5)$$

The subarray output vector $\mathbf{y}$ is then

$$\mathbf{y} = \begin{bmatrix} y_1 \\ y_2 \end{bmatrix} = \begin{bmatrix} \mathbf{0}_{2\times 1} & \mathbf{K}_4 & \mathbf{0}_{2\times 1} \end{bmatrix} \begin{bmatrix} z_3 \\ \kappa_{4,1} \\ \kappa_{4,2} \\ z_4 \end{bmatrix} = \mathbf{R}_3 \mathbf{u}_2. \quad (6)$$

Combining (3) to (6) gives

$$\mathbf{y} = \mathbf{R}_3 \mathbf{R}_2 \mathbf{R}_1 \mathbf{x}. \quad (7)$$

The 2×2 matrix $\mathbf{R}_3\mathbf{R}_2\mathbf{R}_1$ represents the chequered network response from the antenna elements to the subarray ports. Due to reciprocity, reversing the direction of signal flow and finding $\mathbf{x}$ as a function of a stimulus $\mathbf{y}$ results in

$$\mathbf{x} = (\mathbf{R}_3\mathbf{R}_2\mathbf{R}_1)^{\mathrm{T}} \mathbf{y} = \mathbf{R}_1^{\mathrm{T}}\mathbf{R}_2^{\mathrm{T}}\mathbf{R}_3^{\mathrm{T}}\mathbf{y} \quad (8)$$

which shows that the derivation for the reversed signal direction follows the same approach, but uses transposed row transform matrices in reverse order. The scattering parameters between the element and subarray ports are provided by the network response matrix with the scattering parameter S_{y_m,x_n} being element (m, n) of $\mathbf{R}_3\mathbf{R}_2\mathbf{R}_1$.

To find the scattering parameters involving terminated ports, the inter-row signal vector containing the desired terminated port signal must be found, with the signal flow direction depending on whether the scattering parameter is calculated from an element or subarray port. Finding S_{z_3,x_n} and S_{z_4,x_n} in Fig. 4(b) requires applying stimuli at x_n and calculating $\mathbf{R}_2\mathbf{R}_1$ in that order since the signal flow direction is downward. Conversely, S_{z_1,y_1} will be element $(1, 1)$ in $\mathbf{R}_2^{\mathrm{T}}\mathbf{R}_3^{\mathrm{T}}$ since the stimulus is applied to y_1. The parameters S_{z_1,x_n}, S_{z_2,x_n}, S_{z_3,y_m}, and S_{z_4,y_m} are all zero since the corresponding ports are isolated from each other.

The total aperture illumination $\mathbf{x}$ determines the radiation pattern when the feed network is connected to an antenna array. The radiation amplitude pattern, normalised to the array directivity, remains unchanged when $\mathbf{x}$ is multiplied by an arbitrary complex constant $Ae^{j\alpha}$ as only the relative amplitudes and phases of the elements are of importance. Applying an arbitrary constant phase shift α to $\mathbf{x}$ gives

Algorithm 1. Determining chequered layouts.

1) The smallest number of rows that ensures the existence of at least one signal path between the ports y_m and x_n for each non-zero entry $\phi_{m,n}$ in $\mathbf{\Phi}$ is determined.
2) Algorithm 2 is followed in an attempt to find a feasible solution that satisfies the constraints.
3) If no feasible solution is found, one row is added to the network as illustrated in Fig. 3.
4) Steps (2) and (3) are repeated until a feasible solution is found.

$\mathbf{y}e^{j\alpha} = \mathbf{R}_3\mathbf{R}_2\mathbf{R}_1\mathbf{x}e^{j\alpha}$, where $e^{j\alpha}$ can be incorporated into any of the row matrices. This means that any phase shift can be added to or subtracted from all the phase shifts in a row to, for example, reduce the lengths of the transmission lines used as phase shifters.

From the 2×2 chequered network derivation, a simplified procedure can be deduced for deriving the response of any chequered network.

1) Rows are numbered from top to bottom. The inter-row signal vectors are defined with the left-most signal node corresponding to the first element in each signal vector as shown in Fig. 4(b).
2) The row transform matrices are numbered according to their rows and their sizes are determined. Using the signal flow convention in Fig. 4(b), the number of rows in each matrix equals the length of the inter-row signal vector below the row, and the number of columns equals the length of the inter-row signal vector above the row.
3) Each row transform matrix is populated by defining a square block diagonal matrix with the row-specific tile responses $\mathbf{K}_c$ as the block diagonal elements in the order in which they appear in the row. For example, $\mathbf{R}_2$ in (5) is such a block diagonal matrix. If the row transform matrix is rectangular, the block diagonal matrix is padded with zeros to reach the required size.

III. An Algorithm for Designing a Chequered Network to Implement a Desired Response

A. Determining the Network Layout

The procedure to select a layout for a given problem is outlined in Algorithm 1, after which the network can be designed using the approach described below.

B. Single-Stage Optimisation for a Given Set of Constraints

A chequered network implements a desired feed network response $\mathbf{\Phi}$ when the constraints

$$\sigma_m S_{y_m,x_n} = \phi_{m,n} \quad \forall m, n \tag{9}$$

are satisfied, where S_{y_m,x_n} is the scattering parameter between ports y_m and x_n, and σ_m is a complex-valued correction weight applied at subarray port y_m. Additional constraints are added to ensure that the coupling ratios and phase shifts are realisable. After satisfying all the constraints, any remaining degrees of freedom are utilised to minimise the mean power delivered to the terminated ports. The optimisation problem is constraint-driven rather than goal-function-driven in the sense that the network response and realisability criteria are controlled by constraints rather than by the goal function.

The problem described above can be solved using a general-purpose constrained non-linear solver, such as sequential quadratic programming (SQP) [14]. A local solver such as SQP is not guaranteed to converge to a feasible solution, so multiple trial points must be used in an attempt to reach a feasible solution [15]. The MultiStart solver in MATLAB offers a convenient way of starting the SQP algorithm from multiple trial points [16].

The optimisation problem is formulated as

$$\min \left[\sum_l \sum_m \left|S_{z_l,y_m}\right|^2 + \sum_l \sum_n \left|S_{z_l,x_n}\right|^2 \right] \tag{10}$$

with the constraints

$$\mathcal{R}e\left\{\sigma_m S_{y_m,x_n} - \phi_{m,n}\right\} \le \varepsilon \quad \forall m, n \tag{11}$$
$$\mathcal{I}m\left\{\sigma_m S_{y_m,x_n} - \phi_{m,n}\right\} \le \varepsilon \quad \forall m, n \tag{12}$$
$$p_c^2 + q_c^2 = 1 \quad \forall c \tag{13}$$
$$p_{\min} \le p_c \le p_{\max} \quad \forall c \tag{14}$$
$$0 \le q_c \le 1 \quad \forall c \tag{15}$$
$$\psi_{\min} \le \psi_c \le \psi_{\max} \quad \forall c \tag{16}$$

where c are the tile indices. The goal, defined in (10), is to minimise the mean power delivered to the terminated ports from both subarray and element ports. Constraints (11) and (12) ensure that the real and imaginary components of the network response achieve their desired values to within a tolerance ε. The relationship between p_c and q_c is maintained by (13). The fact that p_c and q_c are specified individually instead of expressing q_c as $\sqrt{1-p_c^2}$ allows the algorithm to pass through infeasible regions which improves convergence. The range of coupling ratios is bounded by (14), while (15) ensures that (13) always only has real-valued solutions. The range of phase shifts is bounded by (16).

Q trial points are passed to the MultiStart solver which are uniformly distributed over the bounds (14) to (16), $-1 \le \mathcal{R}e\{\sigma_m\} \le 1$, and $-1 \le \mathcal{I}m\{\sigma_m\} \le 1$. The final solution is the feasible solution with the lowest goal function value.

On transmission, terminated ports that are not isolated from subarray ports (e.g. ports z_1 and z_2 in Fig. 4) may have to dissipate large amounts of power. Constraints of the form

$$\sum_l \left|S_{z_l,y_m}\right|^2 \le P_{\max} \quad \forall m \tag{17}$$

where $P_{\max}$ is the maximum total relative power delivered from a subarray port to the terminated ports, can be placed on the power delivered to terminated ports. However, the scattering parameters assume that only one port is excited at a time, so the actual power delivered to terminated ports will differ when multiple ports are stimulated simultaneously. Furthermore, the power delivered will depend on the signals at the stimulated ports, so the power delivered will vary with steering angle in the case of a beamforming array. Scattering-parameter-based terminated powers therefore do not

reflect the actual losses of a complete beamforming system in operation, but nevertheless provide a useful way of evaluating the efficiency of a chequered network in a manner which is easy to formulate as a constraint.

Constraints are not placed on the powers delivered to terminated ports on reception since non-uniform aperture illuminations may require that significant power be delivered to terminated ports to form the desired illuminations across the elements. The power delivered to terminated ports is a function of the aperture efficiency of the illuminations and is thus not necessarily indicative of the efficiency of the chequered network implementation. However, the aperture illuminations do not prevent the full utilisation of at least one antenna element. The element port with the lowest loss (i.e. with the least power delivered to the terminated ports) can therefore be used to provide an indication of the efficiency of the chequered network implementation on reception. As with all feed networks, an low-noise amplifier (LNA) may be added at each antenna element to improve system performance.

C. Multi-stage Optimisation to Minimise the Range of Coupling Ratios and Phase Shifts

Two observations which arise from the approach outlined above are considered below.

First, the obvious choice when specifying the constraints on the coupling ratios and phase shifts is to specify the worst-case constraints that are tolerable for the chosen hardware implementation. However, it is often possible to find feasible solutions with even more stringent constraints, which is desirable as certain coupling ratios and phase shifts may be easier to implement. Unfortunately, it is difficult to predict the most stringent constraints that will produce a feasible solution for a given layout and $\mathbf{\Phi}$.

Second, some of the couplers may tend toward having $p_c = 1$ when optimising chequered networks without constraints on the coupling ratios, especially for couplers that are connected to terminated ports. This is a result of the algorithm attempting to minimise the power delivered to the terminated ports. Such couplers reduce to 90° phase shifters and will be referred to as shorted couplers. Shorted couplers are desirable as they simplify the implementation and reduce loss by removing terminated ports. Some couplers may also tend toward having $q_c = 1$, resulting in cross-shorted couplers, which comprise two 180° phase shifters that cross one another. Cross-shorted couplers undesirable as crossovers are difficult to implement [17].

These two observations can be used to devise a scheme for finding the most stringent constraints that are able to produce a feasible solution, while allowing the inclusion of shorted couplers to reduce power loss. Instead of formulating a multi-objective optimisation problem, the proposed approach is to sequentially find solutions using the approach in Section III-B with increasingly stringent constraints, while prioritising those constraints that are deemed most important.

The proposed sequential optimisation procedure is described in Algorithm 2. First, the constraints on the coupling ratios are removed and an initial optimisation is performed using Q trial points. The resulting solution is then evaluated and couplers with $p_c > p_{\text{short}}$ are shorted in the following steps by setting $p_c = 1$. For all non-shorted couplers, if the initial solution has more stringent coupling ratios than those corresponding to $p_{\min}$ and $p_{\max}$, the coupling-ratio constraints are altered to match the range of coupling ratios from the initial solution.

Algorithm 2. Optimising chequered networks.

1) An optimisation is performed from Q trial points without constraints on the coupling ratios.
2) Couplers from step (1) with $p_c > p_{\text{short}}$ are shorted.
3) Optimisation is repeated with incrementing $p_{\min}$ and decrementing $p_{\max}$, until no feasible solution is found.
4) Optimisation is repeated with incrementing $\psi_{\min}$, until no feasible solution is found.
5) A final optimisation is performed from Q trial points with the final constraints.

Next, the procedure outlined in Section III-B is followed repeatedly with coupling-ratio constraints that become more stringent with each MultiStart solver run, until no feasible solution can be found within Q trials. At each run, the solver terminates upon finding the first feasible solution. Depending on the chosen priority, the minimum coupling ratio can be incremented first, the maximum coupling ratio can be decremented first, or the furthest of the two from 0 dB at each step can be changed.

A similar procedure is followed for the phase shifts, where the range $[\psi_{\min}, \psi_{\max}]$ is reduced until no feasible solution is found within Q trials. In the sections to follow, $\psi_{\max}$ is fixed and $\psi_{\min}$ is incremented since a less negative phase shift corresponds to a shorter transmission line, although a different scheme could also be employed depending on the type of phase shifter used.

The first trial point of each solver run is the last feasible solution from the previous run, and the remaining $Q - 1$ trial points are randomly distributed as described in Section III-B. After obtaining the final constraints, a final optimisation is performed from Q trial points.

IV. Results for Some Test Cases

The results for a number of test cases are presented below, after a description of the system parameters.

The chequered-network optimisation algorithm was implemented in MATLAB R2018b and run on a computer with two 6-core Intel Xeon E5-2630 processors and 32 GB of memory. Couplers from the initial solution with coupling ratios above 20 dB were shorted, and coupling ratios and phase shifts were varied in 0.1 dB and 5° steps, respectively.

A. 4×4 Butler Matrix

A Butler matrix is an example of a completely overlapped feed network and is a hardware-based implementation of a fast Fourier transform (FFT) [18]. In this section, a chequered network is designed to implement the discrete Fourier transform (DFT) and is shown to approach the optimised Butler matrix (FFT) implementation.

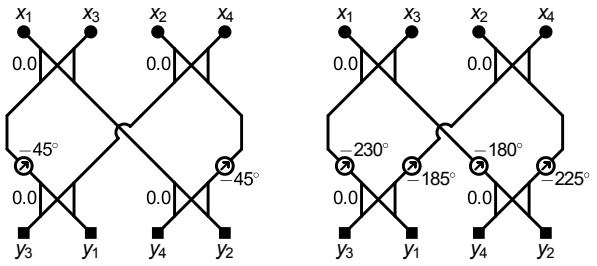

Fig. 5. (a) A 4×4 Butler matrix implementation, and (b) the 4×4 DFT implementation obtained from the proposed algorithm with adjacent phase shifts combined. Coupling ratios in decibels appear to the left of the couplers.

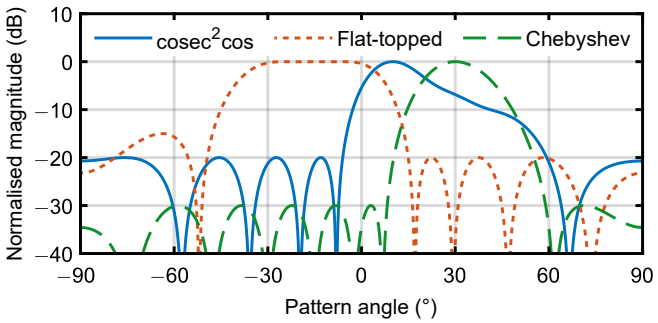

Fig. 6. Radiation patterns of 3 independent subarrays spanning 8 elements.

Fig. 5(a) shows a standard implementation of a 4×4 Butler matrix [19]. In practice, an additional crossover may be required to correctly order ports x_2 and x_3.

The chequered layout was chosen to mirror that of a Butler matrix in anticipation of the network reducing to the standard implementation. The procedure in Algorithm 2 was followed with $\psi \in [-180°, 0°]$, $Q = 20$, and an error tolerance of 10^{-6} on the feed network response. In the same way that couplers with large coupling ratios are shorted, couplers with coupling ratios below −20 dB were constrained to have $p_c = 0$ to allow crossovers in the design as they are present in the standard implementation.

The resulting chequered network is shown in Fig. 5(b), where adjacent phase shifts, including the phase shifts in the shorted and cross-shorted couplers, have been combined. All couplers converged to equal-split couplers.

The design can be further simplified by introducing a phase shift of +185° to ports y_1 and y_3 by changing the phases of the correction weights at these ports, σ_1 and σ_3. Applying the splitting rule [12], the newly introduced phase shifts can be split and shifted up to the two branches containing the −230° and −185° phase shifts, which then become −230° + 185° = −45° and −185° + 185° = 0°, respectively. Applying a 180° phase shift to ports y_2 and y_4 has a similar effect, and the −180° and −225° phase shifts become 0° and −45°, respectively. The resulting simplified design is the same as the standard implementation in Fig. 5(a), thereby validating the proposed algorithm.

B. Three Independent Subarrays Spanning 8 Elements

In order to demonstrate the versatility of the proposed approach, three non-scanning conventional 8-element arrays were designed independently and combined to share the same aperture by means of a 3×8 chequered network. The spacing between elements was half a wavelength.

The specifications of the three arrays were chosen arbitrarily. The first two subarrays were designed using the shaped-beam synthesis algorithm proposed by Orchard *et al.* [20], and five and two pattern roots were placed in the sidelobe and main-beam regions, respectively. The first subarray has a $\text{cosec}^2(\theta)\cos(\theta)$ main-beam shape with its peak at 10° [20] and −20-dB sidelobes. The required beam shape was realised to within ±0.1 dB across $16° < \theta < 48°$. The second array has a flat-topped [20] main beam centred around −15°, with the sidelobes to the left and right of the main beam being −15 dB and −20 dB, respectively. The flat-topped beam was realised to within ±0.01 dB across $-27° < \theta < -4°$. The third subarray is a −30-dB Chebyshev array with the main beam at 30°. The resulting subarray radiation patterns are shown in Fig. 6.

A chequered network was designed to simultaneously implement these three patterns as a fully-overlapped array by using the illuminations of the three subarrays to form the rows of $\mathbf{\Phi}$. Algorithms 1 and 2 were used with with $\psi \in [-180°, 0°]$, $Q = 20$, and an error tolerance of 10^{-3} on the feed network response. Equal priority was given to increasing $p_{\min}$ and decreasing $p_{\max}$ in (14) to minimise the range of coupling ratios as outlined in Section III-C.

Fig. 7 shows the resulting chequered-network design. The final coupling ratios are between −6 dB and 7 dB, and the phase shifts range from −180° to 0°. The antenna element with the lowest loss is at port x_6, from which −3.8 dB of power is delivered to terminated ports z_7 to z_{12}, which gives an indication of the efficiency of the chequered network implementation on reception. On transmission, the total power delivered to terminated ports z_1 and z_2 relative to the input power at the subarray ports y_1, y_2, and y_3 is −4.6 dB, −5.6 dB, and −6.6 dB, respectively. Adding appropriate constraints changes the above powers to −5.0 dB, −6.0 dB, and −5.5 dB, respectively, when constrained to be less than −5 dB.

C. 2×4 Compressive Feed Network

In this section, measured results for a 2×4 narrowband compressive feed network [5] implemented in microstrip for a uniform linear array (ULA) are presented. These are the first published results for a successfully manufactured compressive feed network without hardware constraints on $\mathbf{\Phi}$. The steering range was limited to $|\theta| < 10°$ and the start of the SLL region was $\sin(\theta) = 0.35$. The element spacing was limited to 0.64 wavelengths by manufacturing considerations.

This feed network represents the smallest number of subarrays that constitutes a beamforming array as a single subarray would not allow dynamic control of the array pattern because variations to the single excitation would not affect the array pattern. The limited number of controls thus makes it essential to exploit all the available degrees of freedom if acceptable array performance is to be achieved. Using a compressive feed

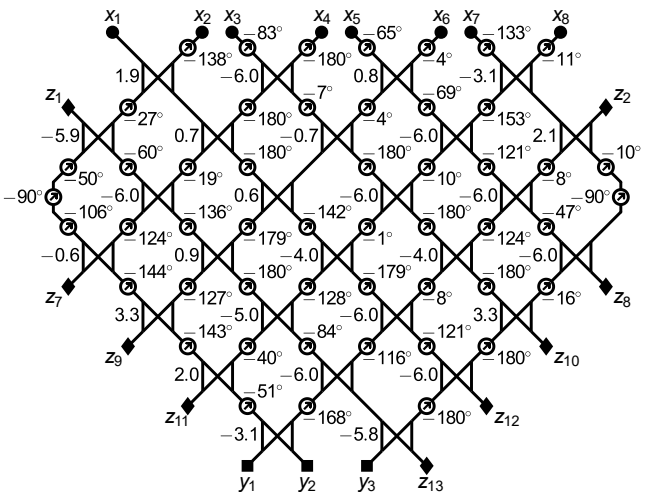

Fig. 7. The obtained design for the 3×8 independent-subarray problem. Coupling ratios in decibels appear to the left of the couplers.

network configuration is therefore desirable, as it places no constraints on $\mathbf{\Phi}$.

Ten independent runs of the compressive array design algorithm [5] all obtained an SLL of −12.15 dB, so all 10 designs were candidates for implementation. Chequered networks were designed using Algorithms 1 and 2 with $\psi \in [-260°,-140°]$, $Q = 20$, and an error tolerance of 10^{-3} on the feed network response. The maximum phase shift was set to −140° to account for the minimum transmission-line length required to connect the couplers. Decreasing $p_{\max}$ was prioritised to avoid the excessively thin microstrip lines which result from large coupling ratios.

Out of the 10 designs, the network which achieved the most stringent constraints while still satisfying the specifications was chosen, with the resulting response of

$$\mathbf{\Phi} = \begin{bmatrix} 0.67\angle 261.6° & 0.35\angle 180.2° & 0.26\angle 126.4° & 0.52\angle 84.9° \\ 0.33\angle 218.8° & 0.51\angle 194.6° & 0.65\angle 213.1° & 0.52\angle 266.8° \end{bmatrix} \tag{18}$$

being implemented by the network shown in Fig. 8. The final coupling ratios are between −4.7 dB and 4.3 dB, and the phase shifts range from −215° to −143°. The phase shifts were not simplified as was done in Section IV-A, showing that Algorithms 1 and 2 produce designs which can be implemented even without additional tuning. The antenna element with the lowest loss (port x_1) delivers −3.6 dB of power to ports z_4 to z_6. On transmission, the power delivered to terminated port z_2 relative to the input power at the subarray ports y_1 and y_2 is −13.2 dB and −8.9 dB, respectively.

The chequered network was implemented in microstrip using single-section branchline couplers [12], with lengths of transmission line being used as phase shifters. The substrate used was Rogers R4003C with a process dielectric constant of 3.38 and a height of 0.81 mm. The manufactured circuit is shown in Fig. 9.

The desired and measured aperture illumination magnitudes and phases at 3.15 GHz are shown in Fig. 10. The

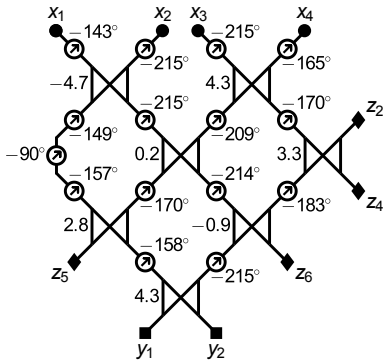

Fig. 8. The obtained design for the 2×4 compressive-feed-network problem. Coupling ratios in decibels appear to the left of the couplers.

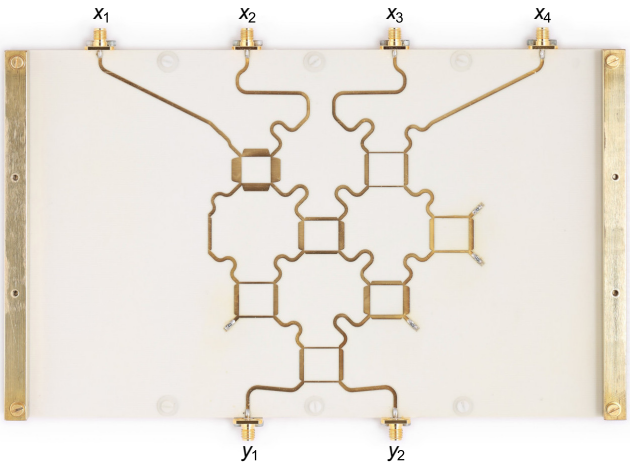

Fig. 9. Photograph of the manufactured 2×4 compressive feed network.

subarray corrections σ_m for the manufactured network were re-calculated to minimise the maximum deviations from the desired aperture illuminations in decibels and degrees. The corrected measured illuminations are within 0.6 dB and 5.2° of the desired response.

The measured frequency-dependent results of the chequered network are summarised in Table I. Fig. 11 shows the worst measured return loss and isolation across all relevant ports. Specifying the required voltage standing wave ratios (VSWRs) as 1.5 and 2 (return losses of 14 dB and 9.5 dB, respectively) gives bandwidths of 4.5% and 14.6%, and isolations of 16.9 dB and 11.2 dB, respectively. Considering a bandwidth of 10% gives a VSWR of 1.65 (a return loss of 12.2 dB) and an isolation of 12.6 dB.

Fig. 12 shows the accuracy with which the manufactured network realises the desired response as a function of frequency. Errors are found by calculating $\sigma_m S_{y_m,x_n} / \phi_{m,n}$ $\forall m, n$. The maximum error is calculated as the range of errors divided by two, which ensures that only the relative amplitude and phase distributions are evaluated because arbitrary amplitude and phase shifts can be introducted as outlined in Section II-C. The standard deviation of the errors is also presented to quantify the distribution of the errors relative to their mean. The accuracy across various frequency ranges is given in Table I. The fact that the system was designed for a single

TABLE I
MEASURED WORST-CASE FREQUENCY RESULTS FOR THE 2×4 COMPRESSIVE FEED NETWORK

	Return loss (dB)	Isolation (dB)	f_l (GHz)	f_u (GHz)	Bandwidth (%)	Response accuracy Max.	Response accuracy St. dev.	Transmit/receive loss (dB) Subarrays	Transmit/receive loss (dB) Element x_1
3.15 GHz	18.1	21.2	3.15	3.15	–	0.6 dB, 5.2°	0.6 dB, 4.5°	1.9	3.7
VSWR $\leq$ 1.5	14.0	16.9	3.07	3.21	4.5	1.4 dB, 10.3°	0.9 dB, 6.3°	2.0	4.0
VSWR $\leq$ 1.65	12.2	12.6	3.00	3.32	10.0	1.9 dB, 17.2°	1.2 dB, 10.6°	2.6	4.5
VSWR $\leq$ 2	9.5	11.2	2.94	3.40	14.6	3.5 dB, 22.9°	2.1 dB, 14.5°	3.2	5.3

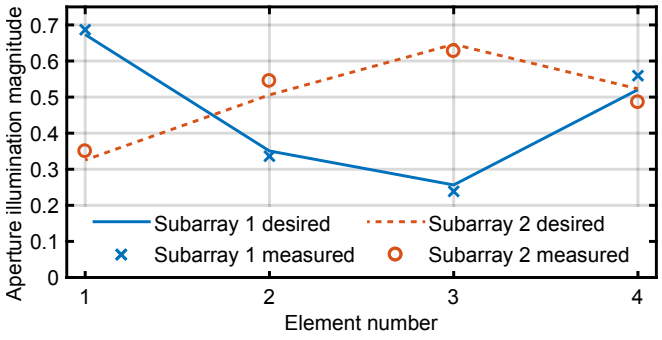

(a)

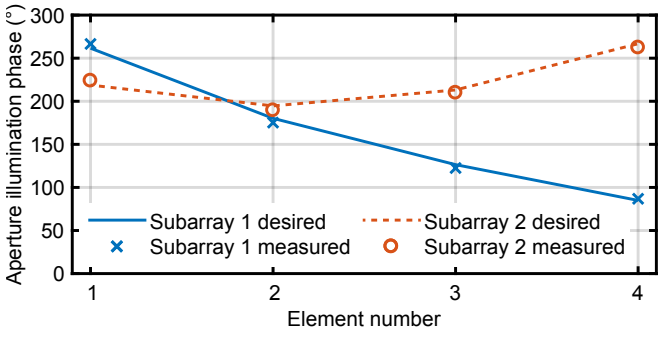

(b)

Fig. 10. Aperture illumination (a) magnitudes and (b) phases for the 2×4 compressive feed network.

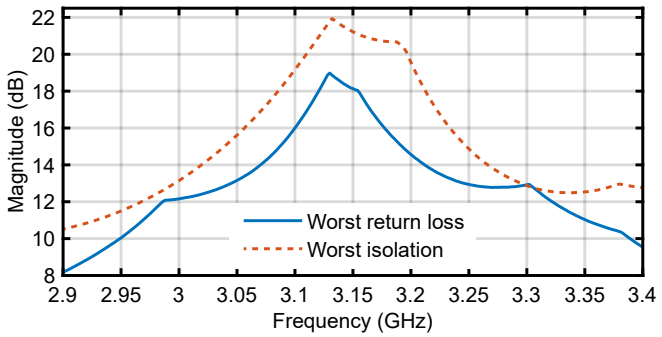

Fig. 11. Measured worst return loss and isolation across all relevant ports for the 2×4 compressive feed network.

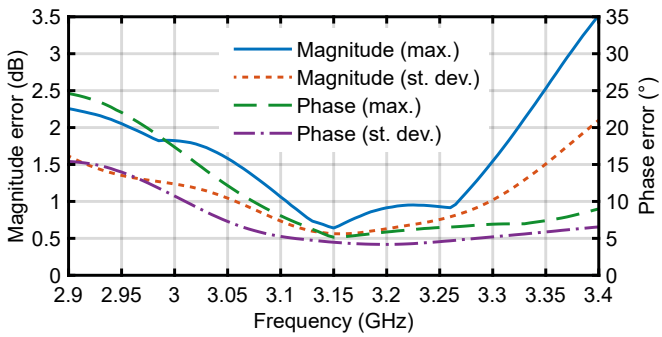

Fig. 12. Measured accuracy of the 2×4 compressive feed network as a function of frequency.

frequency using narrowband components, is seen by the fact that the results are excellent at 3.15 GHz, but deteriorate as the bandwidth is increased. Despite this deterioration, it is believed that the performance at 10% and even 14.6% bandwidth will be acceptable in many applications.

Fig. 13 shows the measured transmit loss from each subarray port to the element ports, and the measured receive loss from the element port with the least loss (x_1) to the subarray ports as a function of frequency. These measurements include the effects of return loss, isolation, power delivered to terminations, and component losses (e.g. due to dielectric loss and finite conductivity). Key results are again summarised in Table I. These results show that the ability to implement an arbitrary feed network comes at the expense of losses which include component losses, which are dependent on the size of the network, and the power delivered to terminations, which depends on the chequered network design.

The results above show that a practical chequered network can be designed and realised despite the many variations inherent in manufacturing. The achieved return loss, isolation and feed network accuracy were reasonable despite manufacturing tolerances, and no manual tuning of the circuit was required. The measured results were achieved without de-embedding the connectors [21], and therefore include the effect of mismatching at the interfaces between the connectors and the microstrip circuit. This shows that chequered networks perform well even when connected to external circuitry via non-ideal interfaces. A chequered network is also able to achieve reasonable results across a range of frequencies despite both using narrowband components and being designed at a single frequency. The presence of terminations in a chequered network can increase losses, but such losses will depend on the network structure and response.

V. CONCLUSION

A network of couplers and fixed phase shifters has been proposed for implementing arbitrary complex-valued feed

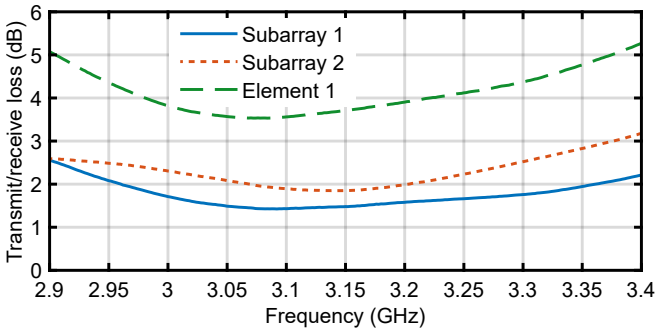

Fig. 13. Transmit loss from subarray ports and receive loss from element port x_1 of the 2×4 compressive network as a function of frequency.

networks. The responses of such chequered networks have been derived using a process based on a series of matrix multiplications. An optimisation approach to determine the coupling ratios and phase shifts required to implement an arbitrary feed network while satisfying constraints necessary to allow the network to be physically implemented has been outlined.

The proposed chequered network and algorithm were validated by demonstrating that a synthesised 4×4 DFT chequered network approaches the manually-designed Butler matrix (FFT) implementation. Three independently designed subarrays were overlapped to share an 8-element aperture (a 3×8 array), illustrating the versatility of the proposed approach. A 2×4 compressive feed network for a ULA was implemented as a microstrip chequered network to demonstrate that complicated unconventional network responses can be realised. The measured aperture illuminations of the microstrip chequered network were within 0.6 dB and 5.2° of the desired aperture illuminations at 3.15 GHz, and within 1.4 dB and 10.3° across the impedance bandwidth of 4.5%. The ability to implement arbitrary feed network responses comes at the expense of losses on transmission and reception, though these losses depend on the network response and structure.

ACKNOWLEDGMENT

The authors would like to thank the anonymous reviewers for their valuable comments and suggestions.

REFERENCES

[1] R. J. Mailloux, *Phased Array Antenna Handbook*. Norwood, USA: Artech House, 2005.
[2] R. J. Mailloux, *Electronically Scanned Arrays*. San Rafael, USA: Morgan and Claypool Publishers, 2007.
[3] S. P. Skobelev, *Phased Array Antennas with Optimized Element Patterns*. Norwood, USA: Artech House, 2011.
[4] J. S. Herd and M. D. Conway, "The evolution to modern phased array architectures," *Proc. IEEE*, vol. 104, no. 3, pp. 519–529, Mar. 2016.
[5] H. E. A. Laue and W. P. du Plessis, "Numerical optimization of compressive array feed networks," *IEEE Trans. Antennas Propag.*, vol. 66, no. 7, pp. 3432–3440, Jul. 2018.
[7] D. Bianchi, S. Genovesi, and A. Monorchio, "Randomly overlapped subarrays for reduced sidelobes in angle-limited scan arrays," *IEEE Antennas Wireless Propag. Lett.*, vol. 16, pp. 1969–1972, Apr. 2017.
[6] T. Azar, "Overlapped subarrays: Review and update [Education column]," *IEEE Antennas Propag. Mag.*, vol. 55, no. 2, pp. 228–234, Apr. 2013.
[8] Z. S. Kachwalla, "A limited-scan linear array using overlapping subarrays," *J. Elect. and Electron. Eng., Australia*, pp. 126–131, Jun. 1983.
[9] J. S. Herd, S. M. Duffy, and H. Steyskal, "Design considerations and results for an overlapped subarray radar antenna," in *IEEE Aerospace Conf.*, Mar. 2005, pp. 1087–1092.
[10] H. Southall and D. McGrath, "An experimental completely overlapped subarray antenna," *IEEE Trans. Antennas Propag.*, vol. 34, no. 4, pp. 465–474, Apr. 1986.
[11] S. M. Duffy, D. D. Santiago, and J. S. Herd, "Design of overlapped subarrays using an RFIC beamformer," in *IEEE Antennas Propag. Soc. Int. Symp.*, Jun. 2007, pp. 1949–1952.
[12] D. M. Pozar, *Microwave Engineering*. Hoboken, USA: John Wiley and Sons, Inc., 2012.
[13] S. P. Skobelev, "Analysis and synthesis of an antenna array with sectoral partial radiation patterns," *Telecommun. Radio Eng.*, vol. 45, no. 11, pp. 116–119, Nov. 1990.
[14] J. Nocedal and S. J. Wright, *Numerical optimization*. New York, USA: Springer-Verlag, 1999.
[15] *Nonlinear Systems with Constraints*, MathWorks Inc., Natick, USA, 2018. [Online]. Available: https://www.mathworks.com/help/optim/ug/nonlinear-systems-with-constraints.html.
[16] *MultiStart*, MathWorks Inc., Natick, USA, 2018. [Online]. Available: https://www.mathworks.com/help/gads/multistart.html.
[17] T. N. Kaifas and J. N. Sahalos, "On the design of a single-layer wideband Butler matrix for switched-beam UMTS system applications [Wireless corner]," *IEEE Antennas Propag. Mag.*, vol. 48, no. 6, pp. 193–204, Dec. 2006.
[18] J. P. Shelton, "Fast Fourier transforms and Butler matrices," *Proc. IEEE*, vol. 56, no. 3, pp. 350–350, Mar. 1968.
[19] W. P. Delaney, "An RF multiple beam-forming technique," *IRE Trans. Military Electron.*, vol. MIL-6, no. 2, pp. 179–186, Apr. 1962.
[20] H. J. Orchard, R. S. Elliott, and G. J. Stern, "Optimising the synthesis of shaped beam antenna patterns," *IEE Proc. H – Microw. Antennas Propag.*, vol. 132, no. 1, pp. 63–68, Feb. 1985.
[21] G. F. Engen and C. A. Hoer, "Thru-reflect-line: An improved technique for calibrating the dual six-port automatic network analyzer," *IEEE Trans. Microw. Theory Techn.*, vol. 27, no. 12, pp. 987–993, Dec. 1979.

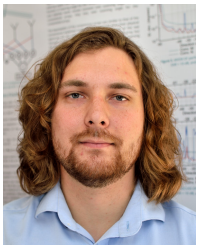

Heinrich Laue (S'16) received the B.Eng. (Electronic) and B.Eng.Hons. (Electronic) degrees, both with distinction, from the University of Pretoria, South Africa in 2015 and 2016, respectively. He is currently pursuing the Ph.D. (Electronic Engineering) degree. His primary research interests are codebook optimisation and the application of compressive sensing (CS) to antenna arrays.

Warren du Plessis (M'00, SM'10) received the B.Eng. (Electronic) and M.Eng. (Electronic) and Ph.D. (Engineering) degrees from the University of Pretoria in 1998, 2003 and 2010 respectively, winning numerous academic awards including the prestigious Vice-Chancellor and Principal's Medal.

He spent two years as a lecturer at the University of Pretoria, and then joined Grintek Antennas as a design engineer for almost four years, followed by six years at the Council for Scientific and Industrial Research (CSIR). He is currently a Professor at the University of Pretoria, and his primary research interests are cross-eye jamming and thinned antenna arrays.